WCAP-18126-NP
Revision 0

June 2017

HiFi™ Cladding for Use in Boiling Water Reactor Fuel

Westinghouse

WCAP-18126-NP
Revision 0

HiFi™ Cladding for Use in Boiling Water Reactor Fuel

Authors*:

Javier E. Romero
Jonathan Wright
Magnus Limbäck

June 2017

Reviewers*: Karin Oldberg
Clara Anghel
Parvez N. Khambatta

Approved*: Edmond J. Mercier, Manager
Product & Plant Licensing

*Electronically approved records are authenticated in the electronic document management system.

Westinghouse Electric Company LLC
1000 Westinghouse Drive
Cranberry Township, PA 16066, USA

EXECUTIVE SUMMARY

This document is the licensing topical report for application of **HiFi** fuel cladding material in boiling water reactor (BWR) nuclear fuel. **HiFi** cladding will be applied to any Westinghouse licensed BWR fuel design.

HiFi material is a zirconium-based alloy designed to maximize the safety margins for BWR fuel, amid increasing demands for higher fuel duties and burnup, by reducing the hydrogen uptake. Initially developed by Nuclear Fuel Industries Ltd. (NFI), a subsidiary of Westinghouse, for use in Japan, **HiFi** cladding has a nominal iron content of 0.4 wt%, which exceeds the upper limit specified for Zircaloy-2 cladding in Reference 6. The benefits of the increased iron content are discussed below. [

]^{a,c}

HiFi cladding refers to the outer component of the fuel cladding. [

]^{a,c}

HiFi cladding is manufactured following the same steps as the current BWR fuel cladding material used by Westinghouse, referred to as Zircaloy-2 LK3. Processing of **HiFi** [

]^{a,c} which are tailored to the modification in chemical composition and to the equipment capabilities of the manufacturers, in order to optimize the microstructure for robust performance. The similar fabrication processes have [

]^{a,c}

Characterization has demonstrated that the as-fabricated microstructure is almost identical between Zircaloy-2 and **HiFi** cladding, [

]^{a,c} This is the origin of the main benefit of **HiFi** cladding, which follows the trend of the industry to maximize the benefit of iron as an alloying element, to [

]^{a,c}

Side-by-side out-of-pile testing comparing **HiFi** and Zircaloy-2 cladding demonstrates that [

]^{a,c} This includes thermal properties, mechanical properties, corrosion properties, and [

]^{a,c} The exception in equivalence between Zircaloy-2 and **HiFi** cladding is the hydrogen pickup fraction observed in **HiFi** cladding, being significantly lower than that of Zircaloy-2 cladding.

Table 1 summarizes the extensive irradiation testing performed [

]^{a,c} In addition to the experience acquired by NFI, Westinghouse acquired relevant experience with [

]^{a,c}

Table 1 Summary of irradiation experience of *HiFi* cladding

[ ]a,c

All the post-irradiation examinations (PIE) have demonstrated that the performance of **HiFi** cladding is equivalent or superior to that of Zircaloy-2 cladding. This includes in-reactor corrosion, hydrogen pickup, creep and growth. Post-irradiation mechanical (yield strength, elongation, fatigue) and [ ]a,c

In particular, current approved models for [ ]a,c Experience has indicated that the benefit of lower hydrogen uptake with **HiFi** cladding becomes apparent in demanding conditions where [ ]a,c

Extensive testing performed on Zircaloy-2 and **HiFi** cladding demonstrates that [ ]a,c This precludes any impact on current approved analysis models and methods.

Having concluded that there are no changes in safety compliance, Westinghouse is seeking NRC approval for the use of **HiFi** cladding [ ]a,c in all approved Westinghouse BWR fuel designs.

TABLE OF CONTENTS

LIST OF FIGURES

LIST OF TABLES

ACRONYMNS, ABBREVIATIONS AND TRADEMARKS

Acronyms and Abbreviations:

AOO	anticipated operational occurrence
bcc	body-centered cubic
BWR	boiling water reactor
CSR	contractile strain ratio
DHC	delayed hydride cracking
ECR	equivalent cladding reacted
EDS	energy dispersive (X-ray) spectroscopy
EOL	end of life
fcc	face-centered cubic
[ ]^{a,c}	[ ]^{a,c}
[ ]^{a,c}	[ ]^{a,c}
HBWR	Halden boiling water reactor
hcp	hexagonal close-packed
HWC	hydrogen water chemistry
K5	Kashiwazaki-Kariwa 5
[ ]^{a,c}	[ ]^{a,c}
[ ]^{a,c}	[ ]^{a,c}
LOCA	loss of coolant accident
LUA	lead use assembly
NFI	Nuclear Fuel Industries Ltd.
NRC	Nuclear Regulatory Commission
NWC	normal water chemistry
[ ]^{a,c}	[ ]^{a,c}
OLNC	online noble chemistry
PCI	pellet-cladding interaction
PIE	post irradiation examination
RIA	reactivity-initiated accident
RXA	recrystallization anneal
SCC	stress-corrosion cracking
[ ]^{a,c}	[ ]^{a,c}
SPP	second phase particle
SRP	Standard Review Plan
TEM	transmission electron microscope (microscopy)
TREX	tube reduced extrusion

Trademark Notes:

1 INTRODUCTION

In order to meet evolving requirements imposed on fuel cladding materials for boiling water reactor (BWR) nuclear fuel, Nuclear Fuel Industries Ltd. (NFI), a subsidiary of Westinghouse Electric Company LLC (Westinghouse) developed **HiFi** cladding, a zirconium-based cladding material that builds on the extensive performance experience acquired with Zircaloy-2 cladding, but with a relatively minor change of the chemical composition. Zircaloy-2 cladding is currently the standard for BWR fuel in Westinghouse. In particular, **HiFi** cladding was designed to improve resistance to hydrogen uptake, intended to maintain and increase safety margins, amid increasing demands for higher fuel duties and burnup.

1.1 PURPOSE

This licensing topical report contains information supporting the application of **HiFi** cladding as fuel cladding in BWR nuclear fuel. Results of extensive testing reported in this document demonstrate that the properties of **HiFi** cladding are equivalent or superior to those of Zircaloy-2 cladding. The purpose is to obtain Nuclear Regulatory Commission (NRC) approval for the application of **HiFi** cladding as fuel cladding material in BWR fuel, [

]^{a,c}

1.2 APPLICABILITY

HiFi cladding refers to the outer component of the fuel cladding and will be applied to any Westinghouse licensed BWR fuel design. [

]^{a,c}

1.3 *HiFi* DEFINITION

HiFi is a zirconium alloy with higher iron content than that specified for Zircaloy-2 cladding, the material currently in use in BWR fuel produced by Westinghouse. Starting in the mid-1980s, NFI developed an advanced cladding material with high corrosion resistance and low hydrogen pickup for next generation high burnup BWR fuel, with discharged average burnup greater than 60 GWd/t. This advanced cladding material has a nominal iron content of 0.4 wt%, which exceeds the upper limit of the ASTM specification for Zircaloy-2 cladding (Reference 6). The new material is called **HiFi**.

Table 1-1 compares the chemical composition of **HiFi** and Zircaloy-2. The final chemical composition of **HiFi** cladding was determined following extensive ex-core testing, aiming to optimize manufacturability, mechanical properties, corrosion and hydrogen pickup. In addition to higher iron, other variants considered during development of **HiFi** cladding included [ ]^{a,c} All the variants demonstrated good fabricability, without significant differences observed during processing. Finally, the composition chosen is that listed in Table 1-1, [

]^{a,c}

Table 1-1 Chemical composition of *HiFi* and Zircaloy-2 alloys

[ ] a,c

Element (wt%)	Zircaloy-2 Alloy
Sn	1.20-1.70
Fe	0.07-0.20
Cr	0.05-0.15
Ni	0.03-0.08
O	0.09-0.16
Zr	Balance

The final heat treatment of **HiFi** cladding is [ ] a,c **HiFi** cladding is manufactured following the same steps as the current Zircaloy-2 cladding used in Westinghouse BWR fuel designs, referred to interchangeably throughout this report as LK3. Processing of **HiFi** cladding has only minimal differences in the specifications of heat treatments and cold pilgering reductions, which have been tailored to the modification in chemical composition, in order to optimize the microstructure for robust performance. **HiFi** cladding is manufactured following the same quality control and testing standards as the current Zircaloy-2 cladding, which exceed stipulations of industry standards such as ASTM B811 (Reference 6). Details of the manufacturing process for **HiFi** cladding can be found in Section 3.1.

1.4 LICENSING BASIS

HiFi cladding is a modification of Zircaloy-2 cladding, which has been achieved by increasing the iron content. The content of this report demonstrates that the properties and performance of **HiFi** are equal to or exceed those of Zircaloy-2. [ ] a,c **HiFi** complies with all design methods and safety analyses that have been approved for Zircaloy-2, and can be employed acceptably in any of the Westinghouse BWR fuel designs in the United States without changes in safety compliance.

Having concluded that there are no changes in safety compliance, Westinghouse is seeking NRC approval for the use of **HiFi** cladding [ ] a,c in all approved Westinghouse BWR fuel designs.

2 BACKGROUND

This section provides perspective and background on the evolution from Zircaloy-2 cladding to **HiFi** cladding, framed in a discussion of basic properties and metallurgy of zirconium based alloys. General metallurgy information in this section comes from References 7 and 8.

2.1 PHASE TRANSFORMATIONS AND MICROSTRUCTURE

For temperatures below about 750°C zirconium is in the so called α-phase, and for temperatures above 1000°C zirconium is in the β-phase. There is a mixed phase region between 750 and 1000°C, which varies depending on the alloy. The α and β phases have hexagonal close-packed (hcp) and body-centered cubic (bcc) crystal structures, respectively. The phase transformation temperatures and the melting point change with variations in alloying composition. These changes depend on the fact that different alloying elements stabilize different phases. For example, in zirconium based alloys tin and oxygen are α-phase stabilizers, while niobium is a β-phase stabilizer. Meaning that, additions of tin and oxygen tend to raise the α to α+β phase transformation temperature, while addition of niobium tends to lower the α to α+β phase transformation temperature. In the Zircaloys the mixed phase region covers the temperature range 750 to 1000°C, and the precipitates are dissolved at about 850°C. [

]^{a,c}

2.2 ALLOYING ELEMENTS

The most common alloying elements used in zirconium-based alloys, relevant for the development of **HiFi** cladding, are briefly discussed in the following subsections.

2.2.1 Oxygen

Oxygen is to be considered as an alloying element, rather than as an impurity. It is added before melting as small additions of ZrO_2 powder. Oxygen is an α-stabilizer, expanding the α region of the phase diagram by formation of an interstitial solid solution. The usual oxygen content in zirconium alloys is in the range of 900-1600 ppm (0.09 to 0.16 wt%) and its purpose is to increase the yield strength by solution strengthening: a 1000 ppm oxygen addition increases the yield strength by 150 MPa at room temperature. The effect is less pronounced above 250°C.

At high concentrations, oxygen stabilizes the α phase up to liquid temperatures. During high temperature oxidation, simulating a reactor accident, a layer of oxygen-stabilized α-zirconium is found between the β-quenched structure and the zirconia. At normal operating temperatures the oxygen diffusion layer ahead of the oxide front is very limited in thickness, e.g., below 1 μm at 400°C. [

]^{a,c}

2.2.2 Tin

Tin is an α stabilizer. It forms, in the α and β phases, a substitutional solid solution. Tin, at a concentration of 1.2-1.7 wt%, was originally added to increase the corrosion resistance, especially by mitigating the deleterious effects of nitrogen in deteriorating the corrosion resistance. Through a better control of processing parameters, and consequently of nitrogen content, it is now possible to reduce the tin content in the current alloys. Tin, however, also has an impact on the mechanical strength of the material and therefore its concentration should not be excessively reduced, without specific consideration of this effect. [ ]^{a,c}

2.2.3 Iron, Chromium, and Nickel

Since iron, chromium and nickel in their phase diagrams give eutectoid decomposition of the β phase they are considered as β-eutectoids.

At the concentrations used in Zircaloy-2 and **HiFi** cladding materials, these elements are fully soluble in the β phase. This temperature of dissolution is in the range of 835-845°C, i.e., in the α+β range. In the α phase their solubility is very low, in the region of 120 ppm for iron and 200 ppm for chromium at the maximum solubility temperature. For the Zr-Cr and Zr-Ni binary alloys, the stable forms of the second phases are Zr_2Ni or $ZrCr_2$. In the Zircaloys, iron substitutes for the corresponding transition metal and the intermetallic compounds found in Zircaloy are $Zr_2(Ni,Fe)$ and $Zr(Cr,Fe)_2$. In Zircaloy-4 alloy, the Fe/Cr ratio of those precipitates is the same as the nominal composition of the alloy. In the **HiFi** alloy, as it occurs for Zircaloy-2, the partitioning of Fe between the two types of intermetallic phases leads to a more complex relationship between nominal composition and precipitate composition, giving a broad range of Fe/Cr ratios in $Zr(Cr,Fe)_2$ and Fe/Ni ratios in $Zr_2(Ni,Fe)$.

The $Zr(Cr,Fe)_2$ precipitates are either hcp or face-centered cubic (fcc), both structures are Laves phases, depending on composition and heat treatment. The equilibrium crystallographic structure depends on the Fe/Cr ratio, fcc below 0.1 and above 0.9, and hcp in between. In common alloys, both types of structure are found, even in the same sample, with random probabilities of occurrences of each. The $Zr_2(Ni,Fe)$ precipitates are a Zintl phase with the body-centered tetragonal structure.

The size of the precipitates is of importance for the properties of the alloys, especially the corrosion rate. Better uniform corrosion resistance is obtained for Zircaloys used in pressurized water reactors (PWRs) if they contain large precipitates, while better resistance to localized forms of corrosion is seen in boiling water reactors (BWRs) in materials that have finely distributed small precipitates. Further discussions regarding the effect of second phase particles (SPPs) on corrosion properties are presented in Section 2.3 below.

2.3 INCREASING IRON CONTENT – SECOND PHASE PARTICLES

Pure zirconium cannot be used in reactor systems due to its mechanical softness and low corrosion resistance in water environments. Present day commercial alloys in general are based on binary, ternary or quaternary alloy systems.

Up to the mid-to-late eighties, to a large extent, only four alloys were used commercially in nuclear systems. Two of these, Zircaloy-2 and Zircaloy-4 alloys, were established by a military program, around 1950. The compositions of these standard Zircaloys, and of two Zr-2.5Nb (Zr with 2.5 wt% Nb) alloys, are defined by ASTM for nuclear applications (Table 2-1, Reference 6). These compositions have remained unchanged for many years. Zircaloy-2 and Zircaloy-4 alloys have been used for cladding and structural materials, such as guide tubes in fuel assemblies and spacers.

Table 2-1 ASTM requirements for contents of alloying elements and some impurities

ASTM Grade	Zircaloy-2 R 60802	Zircaloy-4 R 60804
Sn (wt%)	1.20-1.70	1.20-1.70
Nb (wt%)	-	-
Fe (wt%)	0.07-0.20	0.18-0.24
Cr (wt%)	0.05-0.15	0.07-0.13
Ni (wt%)	0.03-0.08	<0.0070
Fe+Cr+Ni (wt%)	0.18-0.38	-
Fe+Cr (wt%)	-	0.28-0.37
C (ppm)	<270	<270
H (ppm)	<25	<25
N (ppm)	<80	<80
Si (ppm)	<120	<120

The differences between the alloying elements used in the different types of zirconium-based alloys result in different SPPs, or precipitates, or intermetallics. As stated above, SPPs of the type $Zr(Cr,Fe)_2$ are observed in Zircaloy-4 alloy, while the alloying elements in Zircaloy-2 alloy result in two types of precipitates, $Zr(Cr,Fe)_2$ and $Zr_2(Ni,Fe)$.

The effects of the size distribution of the SPPs on the corrosion properties of the Zircaloy materials have been studied extensively, and it has been concluded that the size distribution has an important influence on corrosion behavior. The size of the SPPs depends on the chemical composition and the processing. The alloying elements that form SPPs in Zircaloy-2 and **HiFi** cladding are iron, chromium and nickel. The processing parameters that determine the SPP size distribution are the quenching rate from the β-phase, where these elements are in solid solution, and the subsequent annealing temperatures and times in the α-phase during fabrication.

In BWR conditions, the rate of uniform corrosion is higher when the size of the SPPs is very small. In reactor this effect can be seen at burnups above 20 GWd/t (References 9 and 10). Coarse SPPs may, on the other hand, lead to nodular corrosion in BWRs. [ ] a,c The continuous refinement of Zircaloy-2 has, consequently, led to an iron concentration in the upper range of the ASTM specification in modern BWR applications, [ ] a,c **HiFi** cladding increases the iron concentration even further, resulting in [

] a,c

In addition to the increase in iron content for **HiFi** cladding, [

] a,c

For in-reactor corrosion, it has been shown that the size distribution of the SPPs can be influenced by the fast neutron flux through the acceleration of dissolution processes as well as through the acceleration of alloying elements diffusion within the zirconium lattice (References 9 and 10).

Extensive studies of the effect of SPP size distribution and chemical composition on corrosion and hydriding performance of claddings in BWRs were reported in Reference 10. It was demonstrated that increasing the annealing parameter as well as increasing the iron content resulted in increased mean SPP diameter. The difference in SPP distribution affected both the corrosion and hydriding behavior of the materials. Claddings with smaller initial SPPs showed a higher hydrogen uptake and a lower corrosion resistance than claddings with initially larger SPPs (Reference 10). [

] a,c

Electrochemistry research work on the role of iron on hydrogen pickup mechanisms on zirconium alloys conducted by NFI (Reference 11), has demonstrated that iron addition modifies the surface potential of the material during corrosion, which is an indication of changes in the potential gradient in the oxide film. The potential gradient and differing hydrogen absorption in $Zr(Cr,Fe)_2$ and $Zr_2(Ni,Fe)$ SPPs are theorized to influence the hydrogen (proton) diffusion through the oxide film. Similar modeling and experimental work has proposed a mechanism where the resistivity of the oxide is proportional to the transport of protons, with oxidized alloying elements in the oxide reducing or increasing space charge effects in the oxide, thereby modifying the hydrogen pickup fraction (Reference 12).

The Westinghouse/NFI observations are in line with the results presented in Reference 13, where Zircaloy-2 is compared with materials similar to Zircaloy-2 but with iron and nickel slightly above the ASTM specified values for Zircaloy-2. The results agree with the Westinghouse/NFI experience, and consequently further confirm the advantages gained through the evolution from Zircaloy-2 to **HiFi** cladding.

3 PROPERTIES AND EXPERIENCE

HiFi cladding was developed by NFI, a subsidiary of Westinghouse. Out-of-pile testing was performed during development of **HiFi** cladding, [ ][a,c] Selected candidates were included in irradiation programs in commercial and experimental BWR plants. Irradiation data has been accumulated up to a burnup of 75 GWd/t (see Sections 3.4.1 to 3.4.4). The development program by NFI has also been documented in several publications (References 14 to 18).

In addition to the development program for **HiFi** cladding led by NFI, Westinghouse acquired relevant experience with [ ][a,c]

More recently, Westinghouse qualified [ ][a,c]

Out-of-pile testing results from [ ][a,c] are presented in Section 3.3, together with the combined irradiation experience, demonstrating that the properties and performance of **HiFi** cladding are equal to or exceed those of Zircaloy-2 cladding.

3.1 MANUFACTURING PROCESS

HiFi cladding for Westinghouse nuclear fuel designs is manufactured following the same steps as the current Zircaloy-2 LK3 cladding. Processing of **HiFi** [ ][a,c] which are commonly tailored to the modification in chemical composition and to the equipment capabilities of each manufacturer, in order to optimize the microstructure for robust performance. Table 3-1 lists the basic manufacturing steps for **HiFi** cladding (the same as Zircaloy-2 LK3 cladding). Inspection and intermediate conditioning steps (straightening, cleaning, polishing) are not included in the table, as they are adjusted by each manufacturer to fulfill the material specifications. [ ][a,c]

Table 3-1 *HiFi* cladding manufacturing steps (same steps as Zircaloy-2 LK3 cladding)

[ ]a,c

HiFi ingots, for the outer component of the lined BWR cladding, are melted using [ ]a,c **HiFi** alloy is melted [ ]a,c times to homogenize the distribution of alloying elements. Ingots are forged at high temperature into bars and subsequently β-quenched. For the current cladding designs, **HiFi** [ ]a,c Following the final pilgering, the tubes undergo [ ]a,c For surface finishing, the surface of the inner diameter [ ]a,c

Following melting of the ingots, including control of the chemical composition, a β-quenching operation is performed to homogenize the distribution of alloying elements. The β-quenched microstructure is effectively the starting point for optimization of the SPP size distribution during the subsequent thermo-mechanical processing. The total time at temperature during thermo-mechanical processing following β-quenching is commonly expressed as an annealing parameter, which is defined as (Reference 19):

$$\sum A_i = t_i \, e^{\left(-\frac{Q}{RT_i}\right)}$$

Where t_i represents annealing time (in hours) for annealing step i after β-quenching, T_i is the annealing temperature (K) and Q/R is 40,000 K. It has been demonstrated (Reference 20) that there is a clear correlation between the accumulated annealing parameter and the corrosion behavior of zirconium-based materials, more specifically Zircaloy-2 and Zircaloy-4 alloys. There is also a strong correlation between the size of SPPs and the annealing parameter, independent of the number and the sequence of annealing steps in the α range, which is also not affected by intermediate cold-working steps.

The annealing parameter of **HiFi** cladding [

] a,c

HiFi cladding for Japanese BWR fuel has [

] a,c **HiFi** cladding introduced by Westinghouse in Europe was [
] a,c Table 3-2 shows a comparison of the manufacturing parameters after β-quenching for the different applications of **HiFi** cladding included in this report. [

] a,c

The only difference between **HiFi** cladding for Japan and for Westinghouse is that [

] a,c The table shows how the resulting annealing parameter is [

] a,b,c

Table 3-2 Comparison of nominal manufacturing parameters for *HiFi* cladding

a,b,c

Measurements of SPP size distribution have been performed in **HiFi** cladding manufactured using the different processes described. The variation in mean SPP size is minimal, [ ] a,b,c which is a reflection of the similarities in manufacturing processes. The mean SPP size of modern Zircaloy-2 LK3 cladding has been observed to be [

] a,b,c A difference of this order in SPP size is not expected to result in any detrimental effects on performance, as demonstrated by testing results presented in later sections.

HiFi cladding has also been used in Europe, [

] a,b,c The

inner diameter liner of this **HiFi** cladding [

]a,c

This section has demonstrated that the manufacturing processes used for **HiFi** cladding presented in this document show only minimal differences, driven mainly by the capabilities of different manufacturers. These small differences do not result in significant differences in the resulting annealing parameters and associated microstructures, which demonstrate the equivalence of the manufacturing processes for the new alloy, as well as the closeness to the extensive experience of Zircaloy-2 cladding.

3.2 MATERIAL PROPERTIES

3.2.1 Chemical Composition

For normal production, samples for chemical analysis are taken from the top, middle and bottom of the ingot. For the qualification lot [

]a,c All the results fulfill the requirements of the material specification and the definition of **HiFi** cladding in Section 1.3, and demonstrate the consistency of the chemical composition in the different sections of the ingot and throughout the process. Detailed results are shown in Table A-1 in the Appendix.

3.2.2 Thermal Properties

Relevant thermal properties have been measured for **HiFi** cladding at three different temperatures. In Table 3-3 the thermal properties of **HiFi** cladding are compared to measured or reference values for Zircaloy-2 cladding. The thermal conductivity (λ) of **HiFi** cladding was calculated from measured values of thermal diffusivity (α) and heat capacity (Cp), which were measured using the laser flash method. The thermal conductivity is calculated as $\lambda = \alpha\ Cp\ \rho$, where the density ρ at temperature is calculated from measured thermal expansion.

Reference values for Zircaloy-2 cladding properties were obtained from Reference 21. [

]a,c Table A-2 in the Appendix summarizes the results. [

]a,c

Emissivity depends strongly on the surface condition and the presence of any oxide. A suggested value for standard error of emissivity of 0.1 is found in Reference 22. [

]a,c

Table 3-3 Thermal properties of *HiFi* cladding compared to reference values

a,b,c

3.2.3 Mechanical Properties

Mechanical properties of **HiFi** cladding fabricated for SVEA-96 Optima2 and SVEA-96 **Optima3** fuel, with the Zr-Sn liner, have been tested in order to verify that the material meets the specification of Zircaloy-2 cladding. Tensile and burst tests were performed. The results shown in Table 3-4 fulfill the Zircaloy-2 requirements with margin and are comparable to the experience of Zircaloy-2. Expanded results can be found in Table A-3 and Table A-4 in the Appendix. The reference values in the table correspond to [ ]^{a,c} The differences between the two materials are within the variability of the measurements and the values are well above the minimum specification limits.

Table 3-4 Mechanical properties of *HiFi* and Zircaloy-2 LK3 cladding

a,b,c

3.2.3.1 Thermal Creep

Samples of **HiFi** cladding fabricated for SVEA-96 Optima2 and SVEA-96 **Optima3** fuel were tested [

]^{a,c} For each sample, the diameter was measured before and after each testing time at three axial positions. An average transversal creep strain was then calculated from these three readings. The results are shown in Table 3-5, and are compared with a similar tests performed for Zircaloy-2 LK3 cladding. The results demonstrate that the thermal creep of **HiFi** cladding is [

]^{a,c}

Table 3-5 Thermal creep testing of *HiFi* cladding [ ]^{a,c}

a,b,c

3.2.3.2 Texture and Contractile Strain Ratio

The texture of **HiFi** cladding tubes fabricated for SVEA-96 Optima2 and SVEA-96 **Optima3** fuel was evaluated using laboratory X-ray diffraction. Samples were also tested for contractile strain ratio (CSR), a bulk mechanical parameter related to texture. The CSR obtained for **HiFi** cladding was [

]^{a,b,c} Pole figures from **HiFi** cladding can be found in Figure A-1 in the Appendix.

3.2.4 Material Properties for Fuel Rod Design Methods

The licensed fuel performance codes used for Westinghouse BWR fuel are STAV, VIK, and COLLAPS, approved in Reference 3 and updated to the latest versions in Reference 4. With a change from Zircaloy-2 cladding to **HiFi** cladding, the properties of interest for fuel rod design are the thermo-mechanical properties of the fuel cladding material. Thermo-mechanical properties of zirconium alloys are functions of temperature, burnup and/or fast neutron fluence. The models to describe the material properties used in STAV are described in Appendix A of Reference 3, and supplemented in Appendix A of Reference 4. The following paragraphs review the applicability of these models for **HiFi** cladding, based on these reference works and on the data presented above.

3.2.4.1 Thermal Properties

The thermal conductivity and thermal expansion of zirconium alloys is primarily a function of temperature. Previous work using Zircaloy-2 and Zircaloy-4 materials (Reference 3) demonstrated that the difference between these materials appears to be of the same magnitude as the statistical scatter in the data.

Heat capacity is an auxiliary calculation used for input into transient analysis. For fuel rod design the heat capacity is modeled in the α phase, with a singularity at the phase transformation temperature. The models for thermal properties used for Zircaloy-2 cladding for Westinghouse fuel performance codes are based on MATPRO (Reference 22).

The results in Section 3.2.2 above show [

]^{a,c}

3.2.4.2 Elastoplastic Properties

Correlations for elastoplastic behavior of zirconium alloy cladding are based on MATPRO. Properties such as elastic moduli, Poisson's ratio, strength coefficients, strain rate, and strain hardening are functions of temperature, oxygen content, cold work and fast neutron fluence.

Operational experience and tests on unirradiated and irradiated material, presented in Sections 3.3 and 3.4 below, demonstrate that the mechanical behavior of **HiFi** cladding [

]^{a,c}

3.3 OUT-OF-PILE TESTING

3.3.1 Uniform Corrosion and Hydrogen Pickup

HiFi and Zircaloy-2 tubes [

]^{a,c} The results are shown in Figure 3-1, illustrating that the uniform corrosion resistance of **HiFi** cladding is very similar to that of Zircaloy-2 cladding. More importantly, the in-reactor experience of **HiFi** cladding compared to Zircaloy-2 cladding, presented in Section 3.4, also supports this conclusion.

Figure 3-1 Out-of-pile uniform corrosion testing at 400°C

[ ] a,b,c

Figure 3-2 and Figure 3-3 show the results of hydrogen content and hydrogen pickup fraction after this long term corrosion test. The hydrogen pickup fraction of **HiFi** cladding in autoclave corrosion tests is significantly lower than that of Zircaloy-2 cladding.

Figure 3-2 Out-of-pile hydrogen content

[ ] a,b,c

Figure 3-3 Out-of-pile hydrogen pickup fraction

[ ]a,b,c

HiFi cladding fabricated to the specification for SVEA-96 Optima2 and SVEA-96 **Optima3** fuel [ ]a,c The results shown in Table 3-6 further exemplify a lower hydrogen pickup fraction for **HiFi** cladding with respect to Zircaloy-2 cladding. The distribution of hydrides was verified in the outer component. [ ]a,c as illustrated in Figure 3-4. The orientation of the hydrides matches the experience with Zircaloy-2 LK3.

Table 3-6 Long-term corrosion results for *HiFi* and Zircaloy-2 cladding [ ]a,c

[ ]a,b,c

Figure 3-4 Hydride orientation and distribution after long term out-of-pile corrosion testing of *HiFi* cladding

[ ]a,b,c

3.3.2 Nodular Corrosion

During early development of manufacturing processes for **HiFi** cladding by NFI, the effects of accumulated annealing parameter on nodular corrosion resistance were estimated by ex-core nodular corrosion testing on **HiFi** alloy plates annealed under various conditions. The intermediate anneal after the final solution heat treatment was varied to achieve different accumulated annealing parameters. Coupons made with different annealing parameters were tested in-reactor [ ]a,c for selection of the annealing parameter for **HiFi** cladding.

Plates of manufactured alloys were evaluated for nodular corrosion resistance, by corrosion testing in steam at 525°C for 24 hours. Figure 3-5 shows the results. The nodular corrosion resistance of Zircaloy-2 material is degraded as the annealing parameter $\sum A$ is increased over 10^{-18}, as illustrated by the scatter in weight gain, while **HiFi** material maintains nodular corrosion resistance up to 10^{-17}. [ ]a,b,c

Figure 3-5 Nodular corrosion vs. annealing parameter

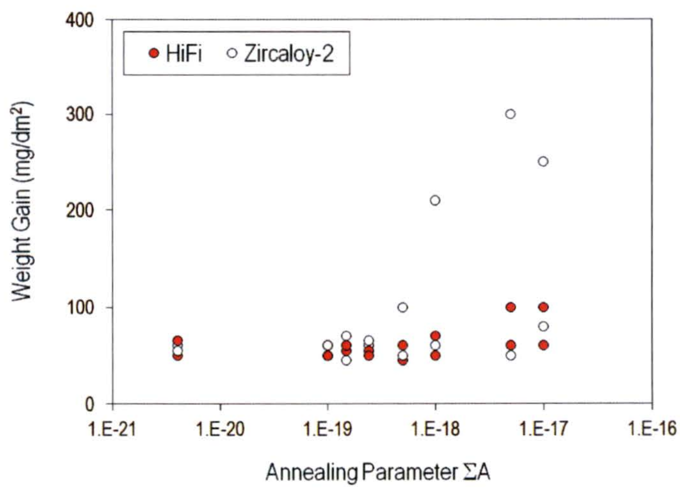

Nodular corrosion tests were performed on [

]a,b,c

Table 3-7 Nodular corrosion test results

[ ]a,b,c

3.3.3 Loss of Coolant Accident Behavior

Out-of-pile tests were performed using **HiFi** cladding tubes fabricated for [ ]a,c to evaluate the loss of coolant accident (LOCA) behavior. Figure 3-6 shows the weight gain as a function of the square root of corrosion time, while Figure 3-7 shows the Arrhenius plot of the parabolic rate law constants determined by high temperature steam oxidation tests. From these results, it was confirmed that the high temperature corrosion behavior of **HiFi** cladding is [

]a,c High temperature burst tests were also performed, and confirmed that the burst behavior for **HiFi** and Zircaloy-2 materials is very similar, as illustrated in Figure 3-8.

Figure 3-6 High temperature steam oxidation

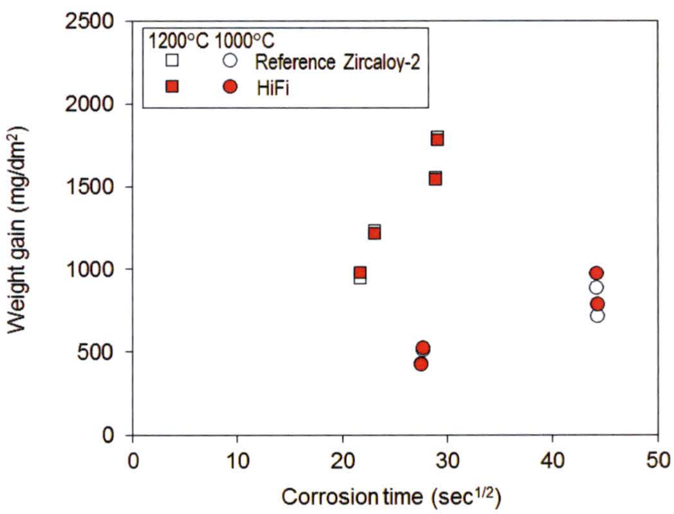

Figure 3-7 High temperature oxidation reaction rate constant (from Reference 18)

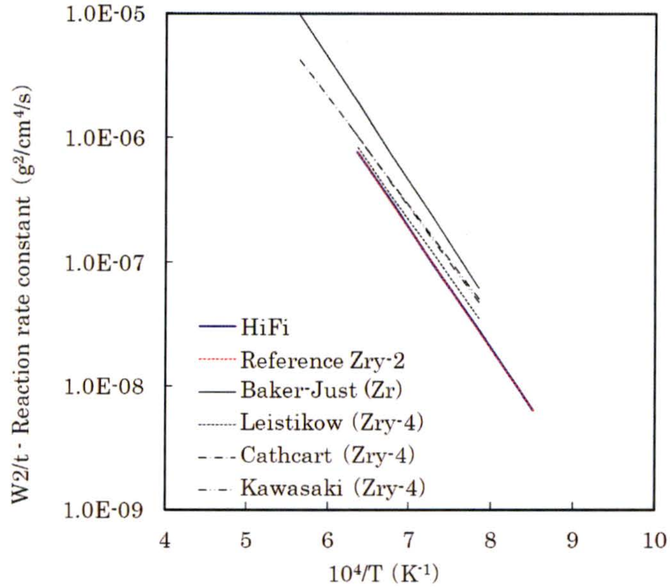

Figure 3-8 Correlation of burst hoop stress and cladding temperature

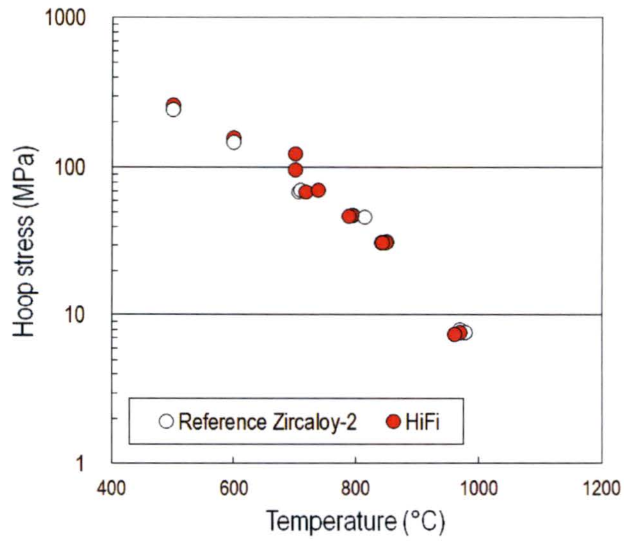

Integral tests simulating LOCA transient conditions and consisting of rod burst, oxidation and re-flooding thermal shock testing of the material were conducted to confirm that the equivalent cladding reacted (ECR) criteria are met (15% in Japan). To address the possible restriction of the cladding shrinkage and the consequent tensile loading, the tests were performed in axial non-restrained and fully restrained conditions during quenching. Figure 3-9 shows the failure map relative to ECR and temperature for **HiFi** and Zircaloy-2 cladding. [

]^{a,c}

Figure 3-9 ECR value measured by quench tests

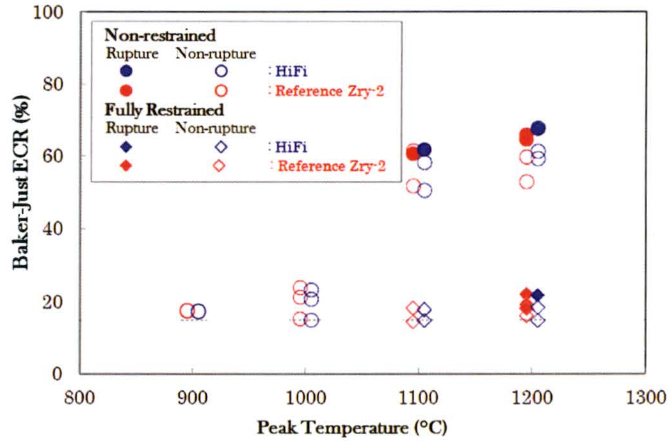

3.4 IRRADIATION EXPERIENCE

In this section, the extensive irradiation experience of **HiFi** cladding in different applications is presented. The purpose is to demonstrate that the in-reactor performance of **HiFi** cladding is equivalent or superior to that of Zircaloy-2 cladding. **HiFi** cladding has been subjected to irradiation in different forms and in different facilities. Irradiation started with coupons in the Kashiwasaki-Kariwa 5 reactor in Japan [ ]a,c The most recent completed irradiation campaigns, [ ]a,c were conducted in [ ]a,c

More recently, Westinghouse SVEA-96 Optima2 fuel rods with **HiFi** cladding were inserted in [ ]a,c Table 3-8 summarizes the irradiation experience for **HiFi** cladding, while the following sections describe the results of the irradiation programs already completed. In all the irradiation programs PIE included both **HiFi** and Zircaloy-2 cladding, in order to compare the performance side-by-side.

Table 3-8 Summary of irradiation experience of *HiFi* cladding

a,c

As described in Section 3.1, **HiFi** material has been manufactured [

]a,c

3.4.1 Plant A - [ ]a,c

Coupons made from **HiFi** and Zircaloy-2 alloys were placed in a container loaded into the water channel of 9x9 fuel in [ ]a,c using the setup illustrated in Figure 3-10. [

]a,c

Coolant was flowed in the container to prevent the coupon surface from boiling. The coupon temperature was estimated as 275°C. The container including the coupons was transported to a PIE facility after three cycles (900 days) irradiation, [ ]a,c Visual inspection, metallographic analysis, hardness and hydrogen analyses were performed. Results show that [

]a,b,c

Figure 3-10 Configuration for irradiation in [ ]a,c

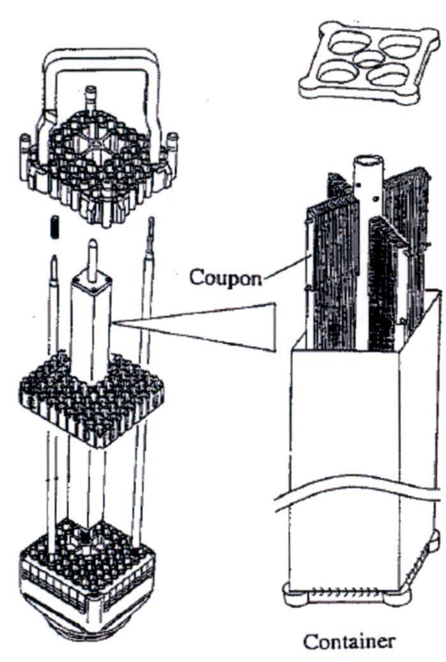

Regarding the relationship between the annealing parameter ∑A and the nodular corrosion resistance, the results were consistent with the ex-core nodular corrosion tests reported in Section 3.3.2. [

]a,b,c

3.4.2 Kashiwazaki-Kariwa 5

The irradiation program in Kashiwazaki-Kariwa 5 (K5) was designed to [

]a,c This large scale program included [

]a,c

Coupons were placed in Zircaloy-2 capsules of 13 mm outer diameter. Capsules were loaded into dummy neutron source holders. Figure 3-11 shows the configuration of the capsules and the corrosion samples as an example. The capsules were irradiated during six irradiation cycles, approximately 2,500 days amounting to an equivalent burnup of 72 GWd/t and fast fluence of $15 \times 10^{25} n/m^2$. Coolant flowed within the capsules; however, coupons surfaces were estimated to be in boiling condition because of γ-heating. According to computer calculations using TRAC code, the void fraction was approximately 20% and the temperature of the coupons was 285°C. The capsule interior was stable and maintained a similar condition during the six cycles. TEM discs were located in an inert atmosphere to avoid oxidation.

The holders containing the coupons were unloaded from the core after [

]a,c They were transported to a post irradiation examination (PIE) facility to perform visual inspection, weight measurement, metallographic examination, hydrogen analysis, mechanical testing and TEM analysis. [

]a,c Figure 3-12 shows the measurements of oxide thickness during irradiation of coupons in K5, together with [

]a,c The proximity of points, even with some overlapping, taken from the side-by-side samples of **HiFi** and Zircaloy-2 tested under the same conditions demonstrates [

]a,c

Figure 3-11 Holder irradiated in K5 and configuration of corrosion sample

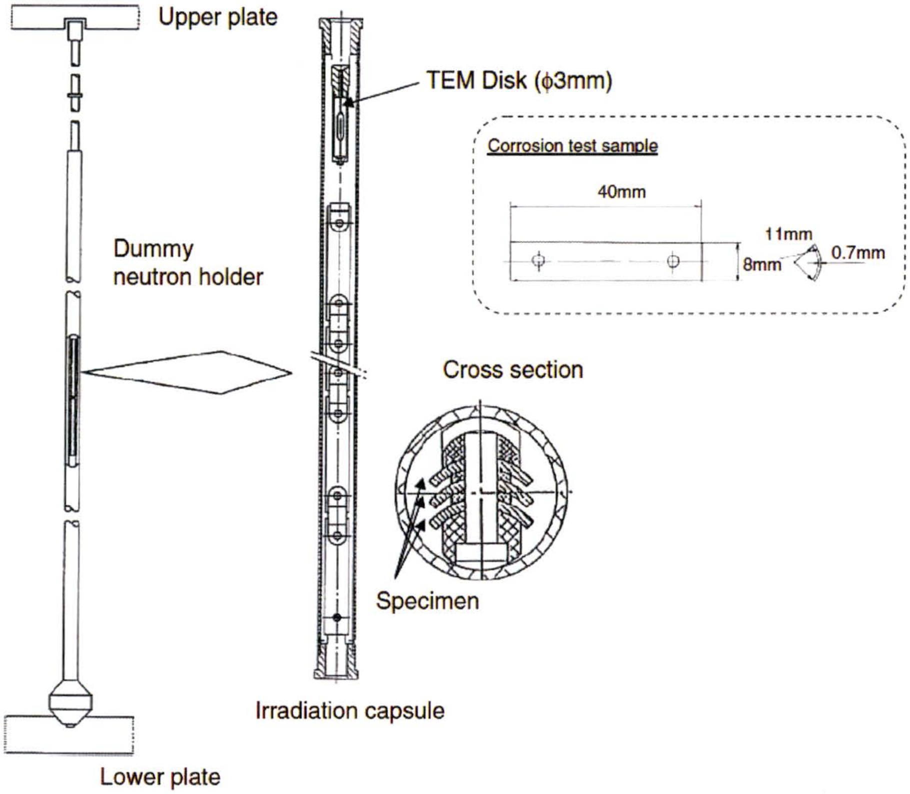

Figure 3-12 Corrosion of K5 coupons and [ ]^{a,c}

[ ] a,b,c

The hydrogen pickup fraction of the K5 coupons is shown in Figure 3-13. Consistent with the out-of-pile tests, the uniform corrosion is comparable between Zircaloy-2 and **HiFi** cladding, but the hydrogen pickup fraction of **HiFi** cladding is significantly lower than that of Zircaloy-2 cladding. Images of hydride precipitation after four cycles of irradiation (47 GWd/t burnup) are shown in Figure 3-14, including the hydrogen content which, given the similar total corrosion, results in an improved hydrogen pickup fraction for **HiFi** cladding. The hydrogen pickup fraction is [

]^{a,c}

Figure 3-13 Hydrogen pickup fraction in K5 coupons

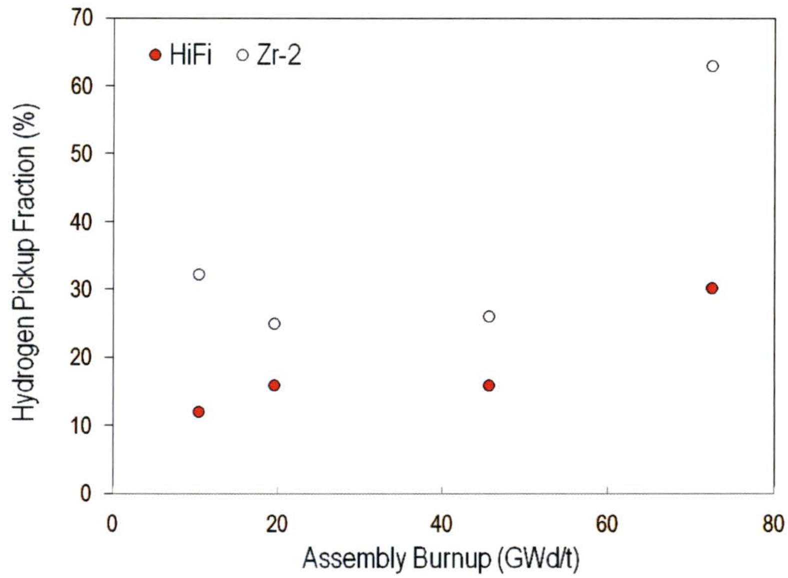

Figure 3-14 Hydride precipitation

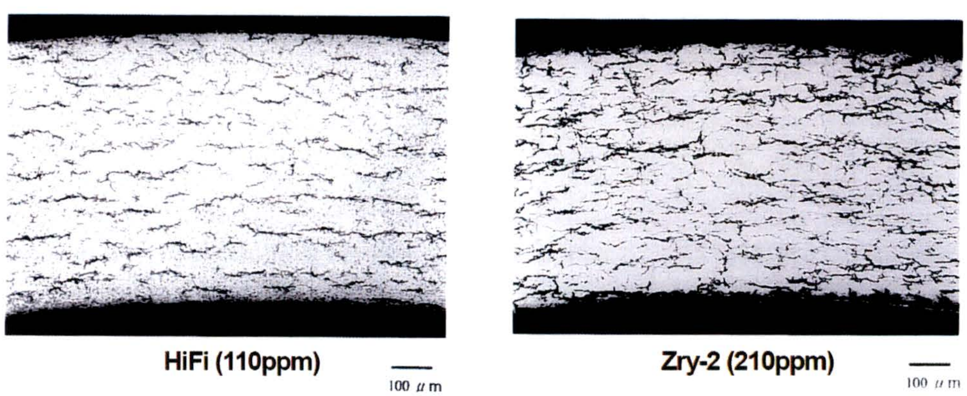

3.4.2.1 Tensile Tests

Tensile tests at 343°C and room temperature were conducted on the **HiFi** cladding and reference Zircaloy-2 cladding coupon samples in K5. The mechanical strength of the **HiFi** coupons showed [ ]^{a,c} which is similar to the experience database illustrating the similarities with Zircaloy-2. Figure 3-15 and Figure 3-16 show the results of yield strength and elongation in K5 for both materials as a function of fluence. The tensile test results, as well as other results in the following sections, are shown together with [

]^{a,c}

Figure 3-15 Yield strength (343°C) of K5 coupons

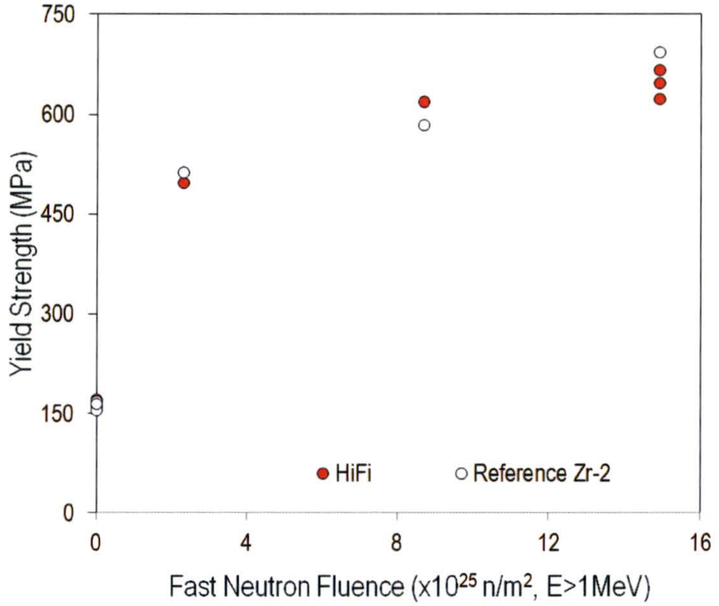

Figure 3-16 Elongation (343°C) of K5 coupons

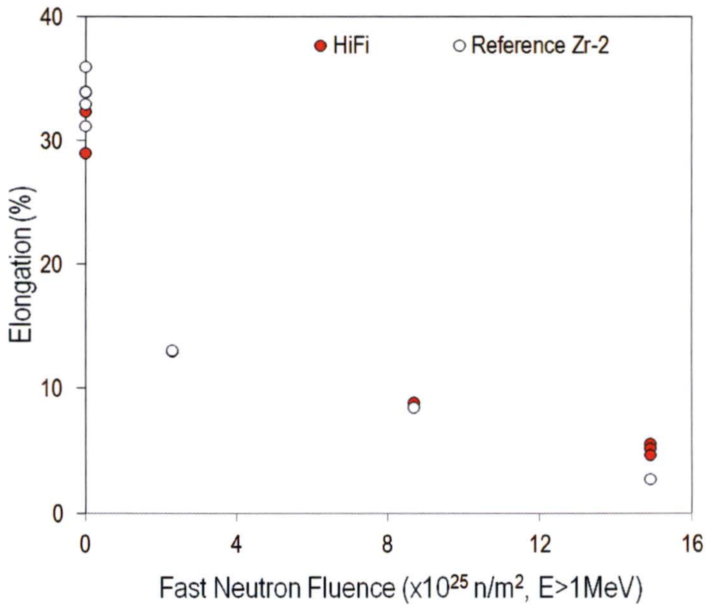

3.4.2.2 Fatigue Tests

Figure 3-17 shows results of fatigue tests performed on unirradiated and irradiated K5 coupons conducted at room temperature, which demonstrate comparable or superior performance, i.e. cycles to failure, of **HiFi** material with respect to the reference Zircaloy-2, for a given stress amplitude. The results for irradiated **HiFi** material exceed the O'Donnell-Langer best fit of unirradiated Zircaloy-2 (Reference 23).

Figure 3-17 Fatigue results of K5 coupons

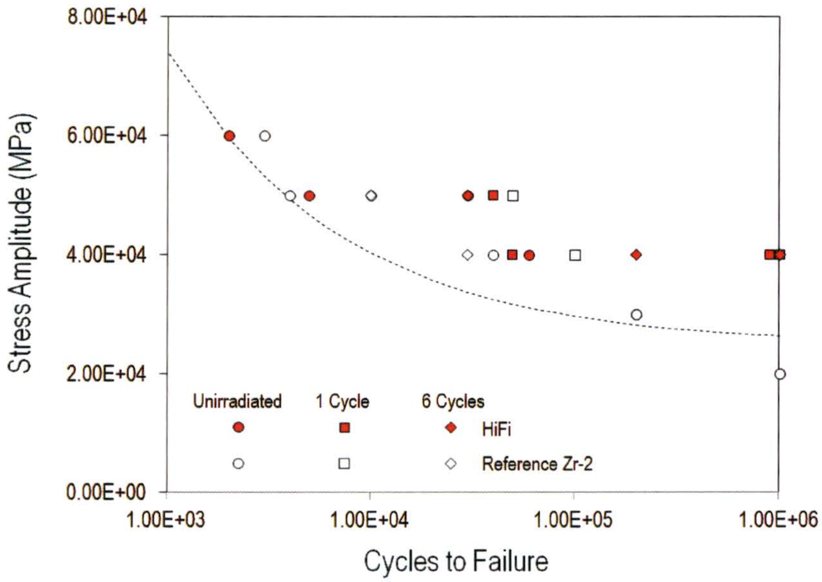

3.4.2.3 Irradiation Creep

Closed specimens pressurized with a noble gas were irradiated in K5 for 1666 days. Figure 3-18 shows outer diameter (OD) measurements performed on these samples, demonstrating [ ]^{a,c}

Figure 3-18 OD measurements in pressurized K5 samples

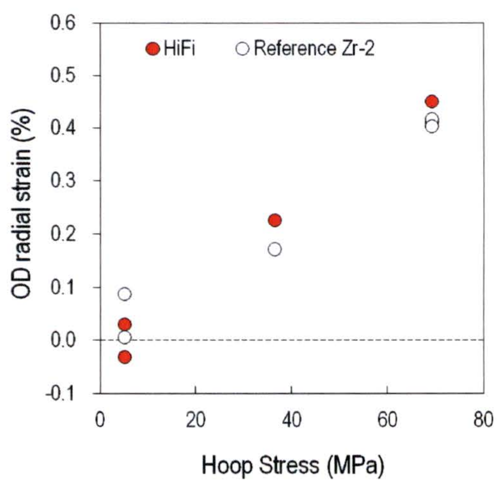

3.4.2.4 Characterization of Second Phase Precipitates

TEM characterization, including energy-dispersive X-ray spectroscopy (EDS) was conducted on **HiFi** and Zircaloy-2 cladding specimens to study the evolution of second phase precipitates. Figure 3-19 shows TEM images of **HiFi** and Zircaloy-2 cladding after six cycles of irradiation. The majority of the precipitates studied appeared amorphous. The presence of iron in the precipitates decreases with irradiation. This is illustrated in Figure 3-20, which shows that the Fe/(Fe+Cr) ratio decreased with neutron fluence. The ratio reaches a stable level, which is slightly higher for **HiFi** material than for Zircaloy-2 material due to the higher iron content.

Figure 3-19 TEM images of precipitates observed in Zircaloy-2 and *HiFi* alloys

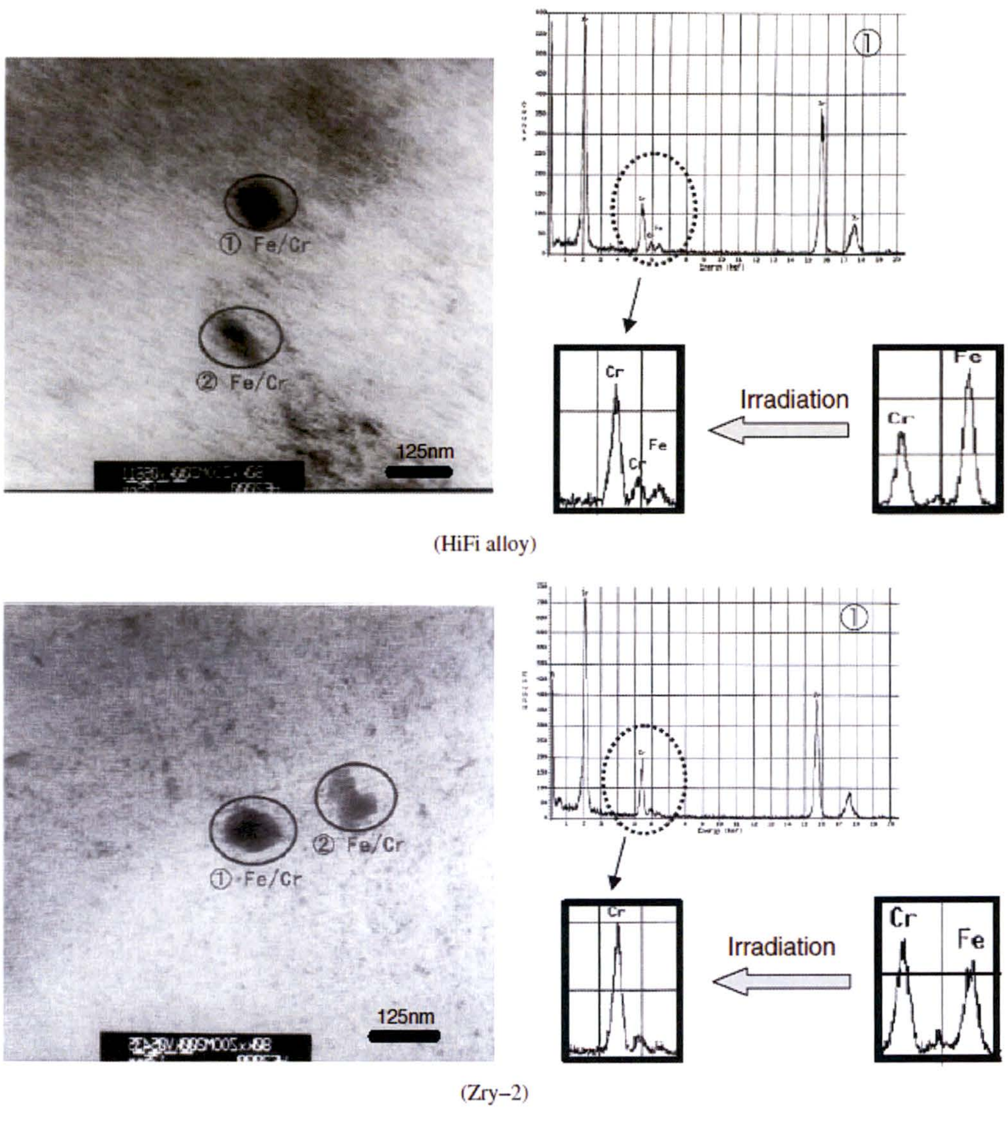

Figure 3-20 Fe/(Fe+Cr) ratio of precipitates as a function of fast neutron fluence

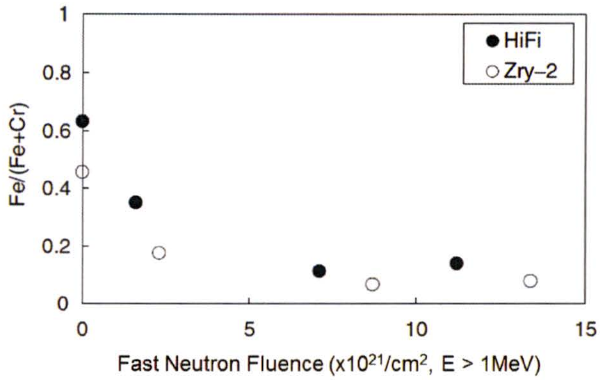

3.4.3 Halden BWR

Irradiation testing of fuel rods with **HiFi** and Zircaloy-2 cladding was performed in a BWR corrosion test loop in the Halden boiling water reactor (HBWR). The fuel rods were irradiated without failure reaching a rod average burnup of 60 GWd/t. The active length of the fuel rods was 40 cm with an outer diameter of 11 mm. Rods were placed in a stainless steel flask as illustrated schematically in Figure 3-21. System pressure of the loop was 7 MPa, coolant inlet temperature was 280°C and the average linear heat generation of the fuel rods was constant, approximately 40 kW/m up to 25 GWd/t and was gradually reduced to 25 kW/m up to 40 GWd/t. Boiling started at 15-20 cm elevation from the bottom of the active length.

Intermediate inspection of the fuel rods was conducted after irradiation to 20 GWd/t and 40 GWd/t fuel rod average. Oxide thickness was measured using eddy current at 40 GWd/t and 60 GWd/t. Results are shown in Figure 3-22 and Figure 3-12. The total oxide thickness observed was between 20 and 60 μm, with thicker oxide observed on the surface oriented closer to the stainless steel flask. Compared to Zircaloy-2 cladding, **HiFi** cladding had a thinner oxide on the surface towards the stainless steel flask. Furthermore, visual inspection showed that the oxide film of the Zircaloy-2 cladding material towards the flask had flaked off, with minimal flaking observed in **HiFi** cladding. Oxide flaking in the Zircaloy-2 material was significant in the non-boiling region of the upstream. The thicker oxide and the flaking can be attributed to the phenomenon known as "shadow corrosion", observed at contact points and/or close proximity regions between zirconium alloy components and other materials such as nickel-based alloy spacers or stainless steel control rods. These results indicate that **HiFi** cladding may be less susceptible to shadow corrosion than Zircaloy-2 cladding.

Figure 3-21 Schematic drawing of Halden BWR corrosion loop test

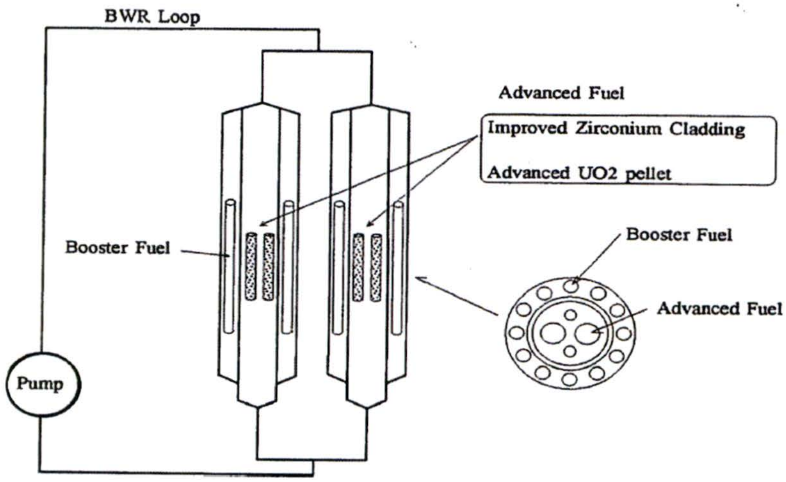

Figure 3-22 Oxide thickness around the circumference of BWR fuel rodlets irradiated in Halden

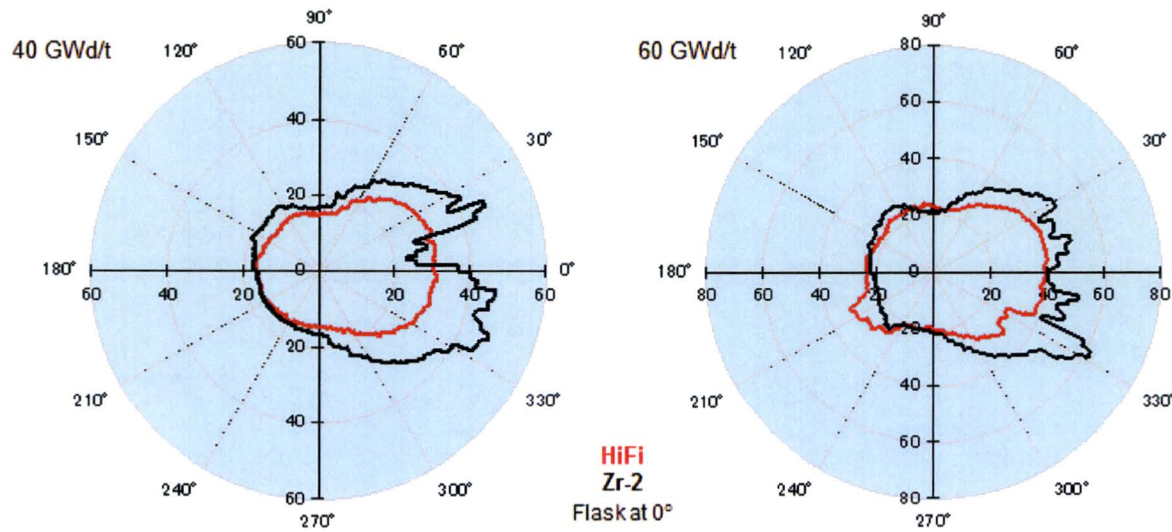

3.4.4 Plant B - [ ]^{a,c}

[ ]^{a,c} fuel assemblies with **HiFi** cladding tubes were irradiated for [ ]^{a,c} reaching [ ]^{a,c} without any issues in performance. In total there were [ ]^{a,c} Six assemblies were discharged after [ ]^{a,c} Two assemblies were irradiated for [ ]^{a,c} The poolside inspection of these assemblies included visual inspection, fuel rod diameter measurements, oxide thickness measurements using eddy current, and fuel rod growth measurements at different points in life. Hot cell examinations included metallography, hydrogen content, hardness, and burst tests.

HiFi cladding tubes were confirmed to be sound by the visual inspection after [ ]^{a,c} as illustrated in Figure 3-23. Average results of measurements of outer diameter of the fuel rods, performed pool-side at two azimuthal positions and along the full length, are shown in Figure 3-24. [ ]^{a,c} Results of fuel rod growth measurements are shown in Figure 3-25, [ ]^{a,c} It is important to note that the [ ]^{a,c}

The oxide thickness of the rods examined is shown in Figure 3-26, [ ]^{a,c} The hydrogen content of the fuel rods, obtained in hot cell, is shown in Figure 3-27. The hydrogen content for [ ]^{a,c} which is combined in the figure. For example, after [ ]^{a,c}

Figure 3-23 Visual inspection results on [ ]^{a,c} fuel rods after [ ]^{a,c} of irradiation

a,b,c

Figure 3-24 OD measurements on [ ]^{a,c} fuel rods

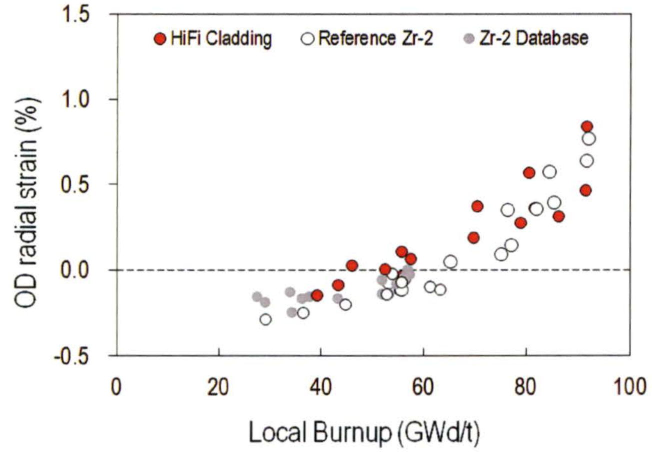

Figure 3-25 Growth of [ ]^{a,c} fuel rods

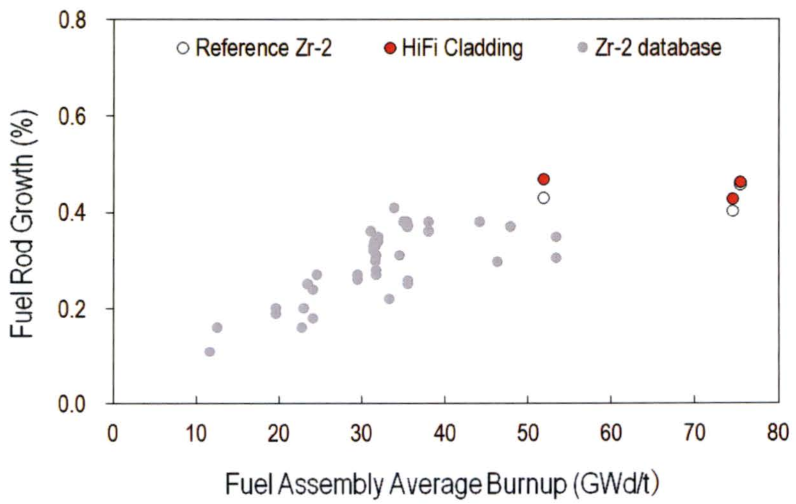

Figure 3-26 Corrosion of [ ]a,c fuel rods

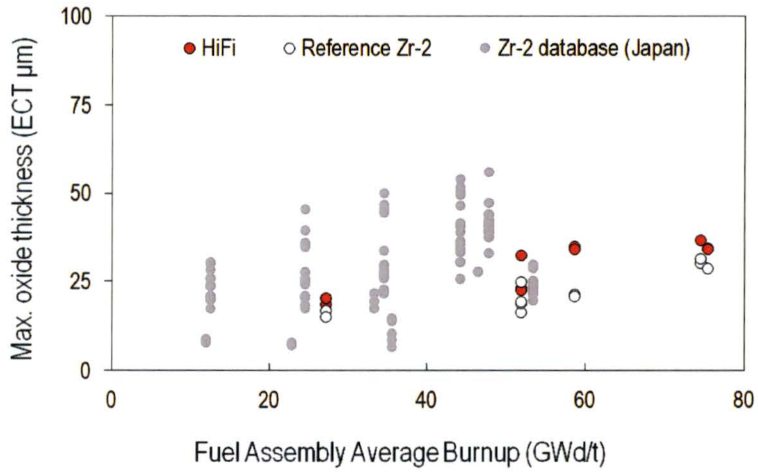

Figure 3-27 Hydrogen uptake of [ ]a,c fuel rods

[ ]a,b,c

Figure 3-28 Hydride distribution of irradiated cladding tubes from [ ]^{a,c} (4 cycles)

HiFi	Reference Zry-2
	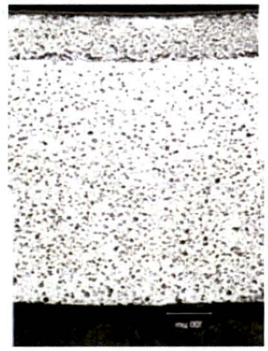

3.4.4.1 Burst Test

Burst tests were conducted to determine the mechanical properties of irradiated **HiFi** cladding tubes. Figure 3-29 and Figure 3-30 show respectively the burst stress and circumference elongation of the cladding tubes at 343°C, showing minimal differences between the **HiFi** cladding and Zircaloy-2. [

]^{a,c}

Figure 3-29 Burst stress of cladding tubes irradiated in [ ]^{a,c}

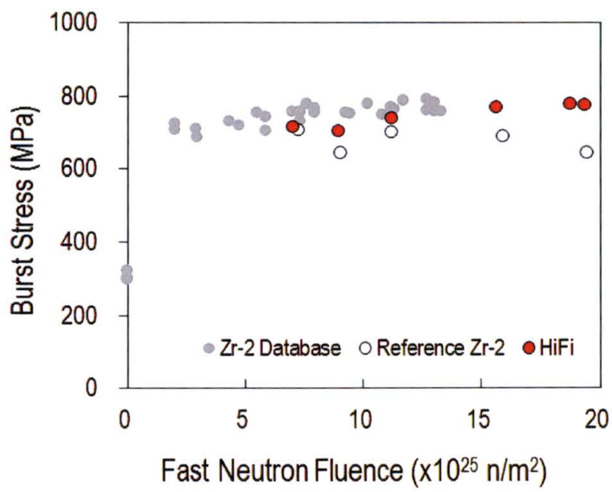

Figure 3-30 Circumference elongation after burst testing of cladding tubes irradiated in [ ]a,c

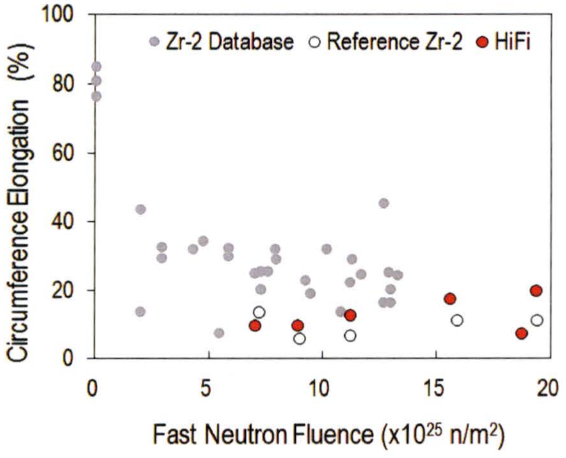

3.4.5 Plant C - [ ]a,c

In parallel to the experience acquired by NFI with **HiFi** cladding in Japan, Westinghouse had started a development program including three different high iron alloys. [

]a,c

Table 3-9 Main alloying elements of [ ]a,c compared to *HiFi* alloy specification

[ ]a,c

In 2001, one fuel assembly was loaded in [

]a,c The fuel assembly was irradiated for [

]a,c Throughout the irradiation program, the fuel rods have been inspected on several occasions, as shown in Table 3-10 below. Results from the pool-side inspections can be found in Figure 3-31 to Figure 3-34. It can be seen that [

]a,c

Table 3-10 Pool-side examinations performed on [ ]^{a,c}

a,c

Figure 3-31 Pool-side rod growth measurements of [ ]^{a,c}

a,b,c

Figure 3-32 Pool-side fuel rod average lift-off of [ ]^{a,c}

a,b,c

Figure 3-33 Pool-side maximum lift-off measured on [ ]^{a,c}

[ ]^{a,b,c}

Figure 3-34 EOL visual pool-side inspection results of [ ]^{a,c}

[ ]^{a,b,c}

In 2012, a rod [ ]^{a,c} This demonstrates that [ ]^{a,c}

3.4.6 Plant D - [ ]^{a,c}

[ ]^{a,c} lead use programs of **HiFi** cladding in Westinghouse fuel are [ ]^{a,c}

[ ]^{a,c} lead use assemblies (LUAs) with [ ]^{a,c} **HiFi** cladding were inserted. As of December 2016, [ ]^{a,c} The

fuel assemblies are [ ]^{a,c}

3.4.7 Plant E – [ ]^{a,c}

The [ ]^{a,c} lead use program of **HiFi** cladding in Westinghouse fuel started in [ ]^{a,c} which broadens the experience window for the exposed materials. In Plant E [ ]^{a,c} fuel assemblies with a total of [ ]^{a,c}

[ ]^{a,c} pool-side PIE of rods with **HiFi** cladding in [ ]^{a,c} Rod growth was [ ]^{a,c} as illustrated in Figure 3-35.

Figure 3-35 Fuel rod growth of rods with *HiFi* and LK3 cladding in [ ]^{a,c}

[ ]^{a,b,c}

4 FUEL DESIGN AND ACCIDENT ANALYSIS

This section discusses fuel design and accident analysis for application of **HiFi** cladding, assessing its effect on approved methods, to verify compliance with 10 CFR Part 50. The Westinghouse methodologies for conducting fuel assembly and fuel rod mechanical evaluations for the current licensed BWR fuel designs, prescribed in Section 4.2 of the Standard Review Plan (SRP) in Reference 24, are detailed in References 1 to 5. This section discusses the different acceptance criteria, concluding that **HiFi** cladding is compliant with approved methods and has acceptable performance in Westinghouse BWR fuel designs. Compliance to approved methods is demonstrated by evaluating the test data.

4.1 FUEL ASSEMBLY MECHANICAL DESIGN

The fuel assembly designs can be impacted by changes in unirradiated yield strength and ultimate strength. The mechanical strength for both irradiated and un-irradiated **HiFi** cladding is [

]^{a,c} Therefore, **HiFi** cladding will meet fuel assembly design criteria.

4.2 FUEL ROD DESIGN

Westinghouse BWR fuel designs are analyzed employing the following design criteria, using the licensed fuel performance code STAV (Reference 4). Each criterion is specified along with the evaluation of the use of **HiFi** cladding on the specific criterion.

4.2.1 Rod Internal Pressure

Criterion: The design criterion for rod internal pressure states that the internal pressure of the fuel rod shall not exceed a value which would cause the outward cladding creep to increase the diametrical fuel pellet-cladding gap. This value of fuel rod internal pressure is defined to be that internal pressure which causes the outward cladding creep rate to exceed the fuel effective swelling rate. This requirement is referred to as "the lift-off criterion".

Evaluation: There is no adverse effect of **HiFi** cladding on the rod internal pressure, irradiation growth, creep or corrosion, compared to Zircaloy-2 cladding. Therefore, there will be no effect on evaluating the lift-off criterion.

4.2.2 Cladding Stresses

Criterion: Fuel rod stresses must be maintained within acceptable limits. This criterion is implemented by establishing design limits for stresses to assure that failure does not occur and that stresses of the fuel rod remain within acceptable limits.

Evaluation: There is no adverse effect of **HiFi** material on unirradiated or irradiated mechanical properties, irradiation growth, creep or corrosion, compared to Zircaloy-2 cladding. Therefore, there will be no effect on evaluating the cladding stresses.

4.2.3 Cladding Strain

Criterion: The total transient induced elastic and plastic cladding circumferential strain should not exceed 1%. In this context, total transient induced strain is the elastic and plastic strain which can occur during normal operation and anticipated operational occurrences (AOOs) excluding the effects of steady-state creep down and irradiation growth.

Evaluation: There is no adverse effect of **HiFi** cladding on the rod internal pressure, unirradiated or irradiated mechanical properties, compared to Zircaloy-2 cladding. Therefore, there will be no effect on the mechanical response for evaluation of the cladding strain.

4.2.4 Hydriding

Criterion: Cladding hydriding from waterside and internal sources shall be maintained sufficiently low that premature cladding failure shall not occur due to hydrogen embrittlement.

Evaluation: There is evidence of the lower hydrogen pickup fraction in **HiFi** cladding with respect to Zircaloy-2 cladding. For the purpose of this Topical Report [

]^{a,c}

4.2.5 Cladding Corrosion

Criterion: Cladding corrosion must be limited to assure that excessive cladding corrosion does not lead to premature fuel rod failures due to excessive metal thinning or excessive cladding temperatures. The effect of cladding corrosion shall be included in the thermal-mechanical evaluation of the cladding.

Evaluation: There is no adverse effect of **HiFi** material on corrosion, as corrosion of **HiFi** cladding has been demonstrated to be [ ]^{a,c} Therefore, there will be no impact on evaluating the cladding corrosion criterion.

4.2.6 Cladding Collapse

Criterion: Cladding collapse shall not occur during the design life of the fuel rod. Cladding collapse or "elastic and plastic instability" refers to the pressure across the tubing walls at which the cladding will buckle in the elastic and plastic ranges.

Evaluation: There is no adverse effect of **HiFi** material on unirradiated or irradiated mechanical properties, irradiation growth, creep or corrosion, compared to Zircaloy-2 cladding. Therefore, there will be no effect on evaluation of cladding collapse. This includes instantaneous collapse at the beginning of life and creep collapse later during operation.

4.2.7 Cladding Fatigue

Criterion: Cladding fatigue shall not cause fatigue damage during normal operation and AOOs. The fatigue evaluation shall account for the effects of cladding corrosion.

Evaluation: [ ]^{a,c} Therefore, there will be no effect of **HiFi** material on the cladding fatigue evaluation.

4.2.8 Cladding Temperature

Criterion: Cladding overheating during normal operation and AOOs shall not cause fuel rod failure.

Evaluation: [ ]^{a,c} and there is no adverse effect of **HiFi** material on the thermal properties of the cladding. Therefore, there will be no effect on evaluation of cladding temperature.

4.2.9 Fuel Temperature

Criterion: The maximum centerline pellet temperature shall remain below the melting temperature of the fuel during normal operation and AOOs.

Evaluation: [ ]^{a,c} Therefore, there will be no effect of **HiFi** material on the fuel temperature criterion evaluation.

4.2.10 Fuel Rod Bow

Criterion: Excessive fuel rod bowing shall be precluded for the design life of the fuel assembly. Fuel rod bowing shall be evaluated, and any significant impact shall be accounted for in the thermal and mechanical evaluation of the fuel rods and the assembly.

Evaluation: There is no adverse effect of **HiFi** material on irradiated mechanical properties, irradiation growth, creep or corrosion, compared to Zircaloy-2 cladding. Therefore, there will be no effect on evaluation of fuel rod bow.

4.3 NUCLEAR DESIGN

There is no effect of **HiFi** alloy on the nuclear design analytical models and methods. [ ]^{a,c}

4.4 THERMAL AND HYDRAULIC DESIGN

The thermal-hydraulic analysis depends on the fuel assembly geometric conditions, the cladding surface finish and the heat transferred to the surface of the cladding. Since the heat transferred to the surface of the cladding remains unchanged, the cladding surface conditions are unaltered, and the fuel assembly geometry remains unchanged, the increase in iron content in the **HiFi** alloy will have no effect on the thermal-hydraulic analysis.

4.5 NON-LOCA ACCIDENT DESIGN

In non-LOCA events the cladding temperature remains below the α to $\alpha+\beta$ phase transition temperature, precluding any significant differences in specific heat. The specific heat, and in general all the thermo-mechanical properties, of Zircaloy-2 and **HiFi** cladding are [

]^{a,c}

4.6 LOCA DESIGN

Thermal conductivity, specific heat, density, thermal expansion and emissivity of **HiFi** material and Zircaloy-2 material are [

]^{a,c}

4.7 PELLET-CLADDING INTERACTION AND REACTIVITY-INITIATED ACCIDENT

Pellet-cladding interaction (PCI) is a stress-corrosion cracking (SCC) phenomenon where an incipient crack is formed at the cladding inner wall, due to high stress combined with the presence of chemically aggressive fission products, and given the right conditions, propagates to the outer wall. The later stages of propagation, where the stress intensity at the crack tip may be very high, can involve other phenomena, e.g., delayed hydride cracking (DHC) or other hydrogen-assisted mechanisms.

The susceptibility to PCI is therefore determined by the properties of the inner wall, i.e., the liner. [

]^{a,c}

The susceptibility of cladding to RIA (reactivity-initiated accident) is determined by a combination of materials microstructure and the hydrogen content. [

]^{a,c}

4.8 HYDROGEN PICKUP

Throughout this report hydrogen data from both unirradiated and irradiated programs have been presented. The complete data set is summarized in Figure 4-1. [

]a,c

Figure 4-1 Summary of hydrogen pickup on *HiFi* and reference Zircaloy-2 cladding

[ ]a,b,c

The benefit of a lower hydrogen pickup with **HiFi** cladding [

]a,c

5 CONCLUSION

Extensive characterization tests performed on Zircaloy-2 and **HiFi** cladding demonstrate that the differences in chemical composition between the materials [ ]^{a,c} The results presented in this document [ ]^{a,c} Therefore, the use of **HiFi** cladding in BWR fuel [ ]^{a,c}

6 REFERENCES

1. "Fuel Assembly Mechanical Design Methodology for Boiling Water Reactors," Westinghouse Report CENPD-287-P-A (proprietary), CENPD-287-NP-A (non-proprietary), July 1996
2. "Fuel Assembly Mechanical Design Methodology for Boiling Water Reactors Supplement 1 to CENP-287," Westinghouse Report WCAP-15942-P-A(proprietary), WCAP-15942-NP-A(non-proprietary), March 2006
3. "Fuel Rod Design Methods for Boiling Water Reactors," CENPD-285-P-A (proprietary), CENPD-285-NP-A (non-proprietary), July 1996
4. "Fuel Rod Design Methods for Boiling Water Reactors – Supplement 1," Westinghouse Report WCAP-15836-P-A (proprietary), WCAP-15836-NP-A (non-proprietary), April 2006
5. "Reference Fuel Design SVEA-96 Optima3," Westinghouse Report WCAP-17769-P(proprietary), WCAP-17769-NP(non-proprietary), November 2013
6. "Standard Specification for Wrought Zirconium Alloy Seamless Tubes for Nuclear Reactor Fuel Cladding," ASTM B811, 2013
7. C. Lemaignan, and A.T. Motta, "Zirconium Alloys in Nuclear Applications," in "Materials Science and Technology – A Comprehensive Treatment," Volume 10B, Nuclear Materials, Part II, Edited by R.W. Cahn, P. Haasen & E.J. Kramer, Volume Editor Brian R.T. Frost, VCH Verlagsgesellschaft mbH, Weinheim (Germany), VCH Publisher Inc., New York, NY (USA), 1994
8. "Waterside corrosion of zirconium alloys in nuclear power plants," IAEA Report, IAEA-TECDOC-996, ISSN 1011-4289, Vienna, Austria, January 1998
9. F. Garzarolli, H. Stehle and E. Steinberg, "Behavior and Properties of Zircaloys in Power Reactors: A Short Review of Pertinent Aspects in LWR Fuel," Zirconium in the Nuclear Industry: Eleventh International Symposium, ASTM STP 1295, 1996, pp. 12-32
10. P. Tägtström, M. Limbäck, M. Dahlbäck, T. Andersson, and H. Pettersson, "Effects of Hydrogen Pickup and Second-Phase Particle Dissolution on the In-Reactor Corrosion Performance of BWR Claddings," Zirconium in the Nuclear Industry: Thirteenth International Symposium, ASTM STP 1423, 2002, pp. 96-118
11. K. Kakiuchi, N. Itagaki, T. Furuya, A. Miyazaki, Y. Ishii, S. Suziki, T. Terai, M. Yamawaki, "Role of Iron for Hydrogen Absorption Mechanism in Zirconium Alloys," Zirconium in the Nuclear Industry: Fourteenth International Symposium, ASTM STP 1467, 2005, pp. 349-366
12. A. T. Motta, R.J. Comstock, A. Couet, "Corrosion of Zirconium Alloys used for Nuclear Fuel Cladding," Annual Review of Materials Research, pp. 311-343 (July 2015)
13. Y. Takagawa, S. Ishimoto, Y. Etoh, T. Kubo, K. Ogata, and O. Kuboto, "The Correlation Between Microstructures and in-BWR Corrosion Behavior of Highly Irradiated Zr-based Alloys," Zirconium in the Nuclear Industry: Fourteenth International Symposium, ASTM STP 1467, 2005, pp. 386-403
14. Itagaki N. et al., "Development of New High Corrosion Resistance Zr Alloy 'HiFi' for High Burnup Fuel," Proceedings European Nuclear Society TopFuel, Wüstzburg, 2003
15. Ohira K. et al., "Recent Experience and Development of BWR Fuel at NFI," Proceedings of the 2005 Water Reactor Fuel Performance Meeting, Kyoto, 2005
16. Kakiuchi K. et al., "Irradiated Behavior for BWR Advanced Zr Alloy (HiFi Alloy)," Proceedings of the 2005 Water Reactor Fuel Performance Meeting, Kyoto, 2005

17. Kakiuchi K. et al., "Irradiated Behavior at High Burnup for HiFi Alloy," Journal of Nuclear Science and Technology, Vol. 43, No. 9, 2006
18. Kataoka K. et al., "The Irradiation Performance and Experience of Advanced Zirconium Alloy HiFi® in a Commercial BWR," Proceedings European Nuclear Society TopFuel, Manchester, 2012
19. M. Dahlbäck, L. Hallstadius, M. Limbäck, G. Vesterlund, T. Andersson, P. Witt, J. Izquierdo, B. Remartinez, M. Díaz, J. L. Sacedon, A.-M. Alvarez, U. Engman, R. Jakobsson and A. R. Massih "The Effect of Liner Component Iron Content on Cladding Corrosion, Hydriding and PCI Resistance," Zirconium in the Nuclear Industry: Fourteenth International Symposium, ASTM STP 1467, 2004, pp. 873-895
20. F. Gazarolli, E. Steinberg, H. Weidinger, "Microstructure and Corrosion Studies for Optimized PWR and BWR Zircaloy Cladding," Zirconium in the Nuclear Industry: Eighth International Symposium, ASTM STP 1023, 1988, pp. 202-212
21. IAEA-TECDOC-1496 "Thermophysical properties database of materials for light water reactors and heavy water reactors," IAEA, Wien, 2006, ISBN 92–0–104706–1
22. NUREG/CR-0497 : MATPRO v11, "A Handbook of Materials Properties for Use in the Analysis of Light Water Reactor Fuel Rod Behavior," February 1979
23. O'Donnell W. J., and Langer B. F., "Fatigue Design Basis for Zircaloy Components," Nuclear Science and Engineering, Vol. 20, 1964, pp. 1-12
24. NUREG-0800, "Fuel System Design Section 4.2," U.S. Nuclear Regulatory Commission Standard Review Plan

A. APPENDIX

Table A-1 Chemical composition of *HiFi* and Zircaloy-2 cladding

[ ] a,b,c

Table A-2 Thermo-physical Properties of *HiFi* and Zircaloy-2 cladding

a,b,c

Table A-3 Tensile testing results for *HiFi* and Zircaloy-2 LK3 cladding a,b,c

Table A-4 Burst testing results for *HiFi* and Zircaloy-2 LK3 cladding a,b,c

Table A-5 Nodular corrosion testing results for *HiFi* and Zircaloy-2 LK3 cladding

a,b,c

Figure A-1 Pole figures from *HiFi* cladding [ ]^{a,c}

[ ]^{a,b,c}